DOI: 10.1002/ejic.200500596

The Bromination of Bulky Trialkylphosphane Selenides $R_2R'PSe$ (R, R′ = *i*Pr or *t*Bu) Studied by Physical and Computational Methods

Cristian G. Hrib,[a] Frank Ruthe,[a] Emma Seppälä,[a] Michael Bätcher,[a]
Christian Druckenbrodt,[a] Cathleen Wismach,[a] Peter G. Jones,[a] Wolf-W. du Mont,*[a]
Vito Lippolis,[b] Francesco A. Devillanova,[b] and Michael Bühl[c]

Keywords: Phosphane selenide dibromides / Heteronuclear NMR / Raman spectroscopy / X-ray structures / Bromine exchange / Ab initio calculations

Bulky trialkylphosphane selenides tBu_3PSe (**1a**), iPr_3PSe (**1b**), $tBu_2(iPr)PSe$ (**1c**) and $tBu(iPr)_2PSe$ (**1d**) react with one equiv. of bromine providing "T-shaped" products $R_2R'P{-}SeBr_2$ (**2a–d**), which contain three-coordinate selenium atoms (10-Se-3). The solid compounds **2b** (bimorphic), **2c** and **2d** exhibit different extents of distortions of the $PSeBr_2$ moieties and different patterns of intermolecular soft–soft interactions. In mixtures containing **1** and **2**, exemplified by the "NMR-titration" of **1c** with molecular bromine, averaged ^{31}P NMR singlets and their ^{77}Se satellites indicate rapid intermolecular bromine exchange reactions (kinetic lability of the Se–Br bonds). Calculations modelling such bromine transfer support nucleophilic attack of R_3PSe ($Se \rightarrow Br$) on an electrophilic Br atom of R_3PSeBr_2. Among the phosphane selenides **1a–d**, $tBu(iPr)_2PSe$ (**1d**) gives the largest ^{77}Se NMR upfield shift and $tBu_2(iPr)PSe$ (**1c**) the lowest, that is, ^{77}Se NMR shifts do not correlate with increasing numbers of *tert*-butyl groups. GIAO-HF/962+(d) calculations on the ^{77}Se NMR shifts of compounds **1** allow correlation of surprising relative deshielding of **1c**, compared with **1b** and **1d**, with its particular population of rotamers (excluding a rotamer with *anti* arrangement of the SePCH moiety in **1c**). Bromine addition to compounds **1** leads to line broadening and extreme deshielding in the ^{77}Se NMR spectroscopy. Reaction of **2b** with bromine leads – inter alia – to P–Se cleavage with *P*-bromination. The structures of **1b**, **2b–d** and $tBu_2(iPr)PBr_2$ (**3c**) were determined by X-ray crystallography. In compounds **2b–d**, intramolecular C–H···Br interactions determine the conformation to a large extent.

Introduction

Phosphane chalcogenides $R_2R'P{=}Y$ (Y = S, Se) are known to act as donors towards dihalogen molecules.[1–4] From phosphane selenides, which are stronger donors than the sulfides, a considerable number of 1:1 adducts $R_2R'PSeX_2$ have been isolated.[5–8] *Molecular* structures have recently been determined for $R_2R'PSeI_2$ (type **A**, [10-I-2], R, R′ = C_6H_5, NMe_2, NEt_2,[6] and R = *t*Bu, R′ = I)[7] and for R_3PSeBr_2 (type **B**, [10-Se-3] R, R′ = NMe_2, C_6H_{11}).[8] Ionic structures of solid 1:1 adducts of phosphane selenides with iodine involve $(R_3PSe)_2I^+$ cations with I_3^- (type **C**, [10-I-2]),[5,9,10] whereas R_3PSeI^+ cations (type **D**) are formed as polyiodide salts (Scheme 1).[3,9,11]

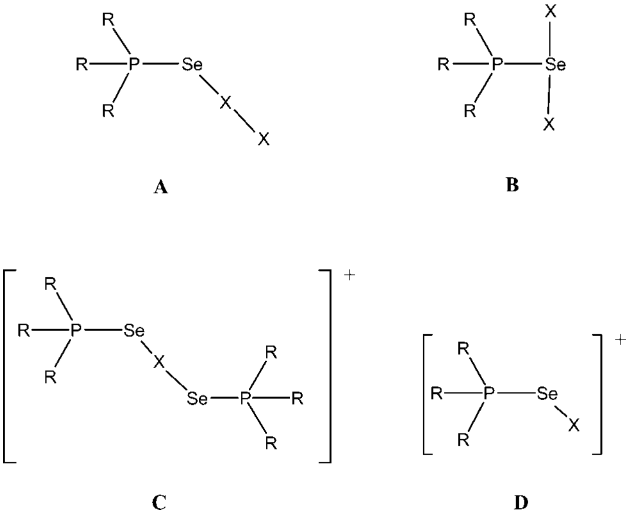

Scheme 1. Various structures of halogen adducts of phosphane selenides.

---

[a] Institut für Anorganische und Analytische Chemie der Technischen Universität Braunschweig,
Postfach 3329, 38023 Braunschweig, Germany
Fax: +49-531-3915387
E-mail: w.du-mont@tu-bs.de
[b] Dipartimento di Chimica Inorganica ed Analitica, Complesso Universitario di Monserrato, Università degli Studi di Cagliari,
S.S. 554 Bivio per Sestu, 09042 Monserrato (CA), Italy
Fax: +39-0706754456
E-mail: devilla@unica.it
[c] Max-Planck-Institut für Kohlenforschung,
Kaiser-Wilhelm-Platz 1, 45470 Mülheim/Ruhr, Germany
Fax: +49-306-2996
E-mail: buehl@mpi-muelheim.mpg.de

Averaged ^{1}H-, ^{13}C- and ^{31}P-solution NMR singlet signals (including their ^{77}Se satellite doublets) and spectra, however, suggest that equilibrium mixtures of several species are present in solutions of such 1:1 adducts.[5,7,9] Until now, no reports on ^{77}Se NMR spectra of phosphane selenide halogen adducts have appeared in the literature. It was observed that addition of a few percent of iodine to a phosphane selenide solution leads to extreme broadening of the ^{77}Se NMR doublet signal and after further addition of iodine, the ^{77}Se NMR signal is no longer resolvable. In the context of the present discussion on theoretical descriptions of the addition of halogens and interhalogens to P=Se or C=Se bonds, it would be desirable to study hypervalent selenium products and their dynamics in solution by ^{77}Se NMR spectroscopy. The present study was undertaken to follow for the first time the course of stepwise bromination of three related bulky trialkylphosphane selenides in solution by ^{31}P and ^{77}Se NMR spectroscopy and to elucidate the role of steric effects that might determine the nature of the products. In the case of phosphane selenide–iodine reactions, slight variations of the substituents attached to phosphorus determined – in an surprising way – the nature of the 1:1 adducts (*molecular* vs. *ionic*)[5,8,9] and the particular supramolecular structures of polyiodide salts from $[R_2R'PSeI]^+$ cations.[9,11]

Reactions

Formation of "1:1 Adducts"

Adding Br_2 in titration-like fashion to solutions of phosphane selenides $R_2R'P{=}Se$ (**1a**: R, R′ = *t*Bu; **1b**: R, R′ = *i*Pr; **1c**: R = *t*Bu, R′ = *i*Pr; **1d**: R = *i*Pr, R′ = *t*Bu) in dichloromethane leads to only one averaged ^{31}P NMR signal, with a pair of ^{77}Se satellites, in all ^{31}P NMR spectra of such solutions. The magnitude of $^1J(^{77}Se,^{31}P)$ decreases with increasing amounts of Br_2; in CD_2Cl_2 the magnitudes of $^1J(^{77}Se,^{31}P)$ are smaller than in comparable C_6D_6 solutions. ^{77}Se NMR resonances of bromination products cannot be resolved as easily as those of the parent phosphane selenides. Adding less than 5% Br_2 to the solution of any of the trialkylphosphane selenides **1** leads to severe broadening of the ^{77}Se NMR doublet signal, which is shifted slightly to a lower field compared with pure **1**. With larger amounts of Br_2 the ^{77}Se NMR signal becomes too broad to be resolved. CD_2Cl_2 solutions of pure *i*Pr$_3$PSeBr$_2$ (**2b**) and *t*Bu(*i*Pr)$_2$PSeBr$_2$ (**2d**), however, allow resolution of ^{77}Se NMR doublet signals, and *t*Bu$_2$*i*PrPSeBr$_2$ (**2c**) gives a single broad ^{77}Se resonance (all about 900–1000 ppm downfield from the parent phosphane selenides) (Table 1). These observations suggest kinetic lability of R_3PSe/Br_2 systems, involving exchange reactions that are *fast* at the ^{1}H, ^{13}C and ^{31}P NMR timescales (and *medium* at the ^{77}Se NMR timescale). Crystallisation of products from **1** with Br_2 provides solids $R_2R'PSeBr_2$ (**2a–d**). In each of these compounds, bromine has been oxidatively added to selenium, which becomes "hypervalent" (structure type **B**, 10-Se-3) (vide infra).

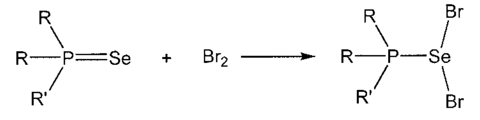

1a: R, R′ = *t*Bu; **1b**: R, R′ = *i*Pr;
1c: R = *t*Bu, R′ = *i*Pr; **1d**: R = *i*Pr, R′ = *t*Bu

2a–d

Reactions with Excess Bromine

Addition of another equivalent of molecular bromine to the dibromides **2b** and **2c** led to their complete consumption in favour of unselective formation of new species. ^{31}P NMR spectra of such a reaction mixture recorded immediately after addition of Br_2 to solutions of **2b** allowed the detection of a singlet ($\delta\,^{31}P = 72.7$ ppm) with satellites exhibiting a coupling constant $^1J(^{77}Se,^{31}P)$ of ±499 Hz (5% smaller than that of **2b**). Isolating crystals from such a solution led, however, to a second polymorph of compound **2b**, and to crystals that apparently contain *i*Pr$_3$PBr$^+$ cations, accompanied by severely disordered cationic P–Se species, and by bromoselenato(IV) anions ($SeBr_6^{2-}$ and $Se_2Br_9^-$). The CH_2Cl_2 solution from these crystals gives a ^{31}P NMR signal (δ = 71 ppm) with $^1J(^{77}Se,^{31}P)$ = ±506 Hz, accompanied by the singlet signal of *i*Pr$_3$PBr$^+$ (δ = 113.9, no ^{77}Se satellites).[12,13] As reference compounds for the bromination products, *i*Pr$_3$PBr$_2$ (**3b**)[12,13] and *t*Bu$_2$(*i*Pr)PBr$_2$ (**3c**) were prepared and characterised. Solid **3c** consists of ion pairs with weak Br···Br interactions. An attempt to generate the *i*Pr$_3$PSeBr$^+$ cation from **2b** by bromide abstraction with $HgBr_2$ in CH_2Cl_2 solution led after two days to a mixture of products ($\delta\,^{31}P$ 75 [very broad, $W_{1/2}$ about 85 Hz], $\delta\,^{31}P$ = 80.0 [satellite doublet J = ±430 Hz], 94.2 and 113.8). From this solution a single crystal of $[iPr_3PSe_3PiPr_3]^{2+}[Hg_2Br_6]^{2-}$ (**4**) was obtained.[13b]

Table 1. Addition of bromine to **1b** and to **1c** followed by NMR (*J* values are in italics).

Solution (CD_2Cl_2)	$\delta\,^{31}P$ [ppm]	$^1J(^{77}Se,^{31}P)$ [Hz]	$\delta\,^{77}Se$ [ppm]	$^1J(^{77}Se,^{31}P)$ [Hz]
*i*Pr$_3$P=Se	70.6	692	–481.5	690
*i*Pr$_3$P=Se + Br$_2$	69.8	521	409.0	521
*i*Pr$_3$P=Se + 5Br$_2$	72.7	499	–	
*t*Bu$_2$*i*PrP=Se	84.4	696	–399	692
*t*Bu$_2$*i*PrP=Se + 0.05 Br$_2$	83.7	687	–381	689
*t*Bu$_2$*i*PrP=Se + 0.10 Br$_2$	83.6	682	–358, – (broad, ≈700±40)	
*t*Bu$_2$*i*PrP=Se + Br$_2$	82.9	520	–	

^{31}P and ^{77}Se NMR Spectra

Trialkylphosphane selenides ($R_3P{=}Se$) exhibit increasing ^{31}P downfield shifts with increasing α-branching of the alkyl groups to a lesser extent than do their parent trialkylphosphanes (R_3P) (Table 2).[15b] As expected, the ^{31}P signal of the mixed-substituted compounds tBu$_2$(iPr)PSe (**1c**) [δ^{31}P = 79.2 and tBu(iPr)$_2$PSe (**1d**) (δ = 85.8 ppm)] appears downfield from **1b** (δ = 72.2 ppm) but upfield from **1a** (δ = 94.7 ppm). Compared with their parent phosphanes $R_2R'P$, the ^{31}P resonances of phosphane selenides **1a**–**d** appear 30–50 ppm downfield, but the bromine addition products $R_2R'PSeBr_2$ (**2a**–**d**) appear slightly upfield from their respective selenides **1**. *Stepwise* addition of bromine to **1a**–**d** does not lead to new ^{31}P NMR signals of reaction products; the singlet signals are only shifted slightly upfield towards those of pure **2a**–**d**.

More indicative of the reaction course of phosphane selenides with electrophiles are coupling constants $^1J(^{77}\mathrm{Se},^{31}\mathrm{P})$, which are determined from satellite doublets in the ^{31}P NMR spectra. The magnitudes of ^{77}Se,^{31}P coupling constants of **1a**–**c** are comparable to those of $Me_3P{=}Se$ or $Et_3P{=}Se$.[14,15b] These couplings are solvent-dependent, being about 2–3 % smaller in polar solvents (e.g. acetonitrile, dichloromethane) than in benzene.[16,17]

With increasing amounts of added bromine, the ^1J values decrease continuously from about 700 ± 15 Hz (in the starting materials) to about 525 Hz in the 1:1 products with bromine.

In the ^{77}Se NMR spectra (Table 3), a straightforward correlation (like that of δ^{31}P) between chemical shifts of $R_3P{=}Se$ and increasing α-branching of the alkyl groups in **1a**–**d** does not exist. From comparison of $Me_3P{=}Se$ (δ^{77}Se = –235[14]) via $Et_3P{=}Se$ (δ^{77}Se = –428[15b]) to iPr$_3$P=Se (**1b**, δ^{77}Se = –484[15b]), upfield shifts may be correlated with increasing α-branching. However, exchanging two iPr groups of **1b** for two tBu groups (in **1c**) does not lead to a further monotonic increase of δ^{77}Se (see Table 1). A comparable unexpected ^{125}Te NMR deshielding of tBu$_3$P=Te,[15a] compared with iPr$_3$P=Te, has already been recognised,[15b,16] but a conclusive explanation has not yet been given; as in the above $R_3P{=}Se$ series, the ^{125}Te resonance of tBu(iPr)$_2$P=Te appears further upfield than that of iPr$_3$P=Te, whereas the ^{125}Te signals of the following members of the series (tBu$_2$-iPrP=Te and tBu$_3$P=Te) appear at significantly lower fields.[18]

Calculations of ^{77}Se NMR Shifts

For a deeper understanding of the unexpected variation of magnitudes of δ^{77}Se and of δ^{125}Te in these sterically crowded phosphane chalcogenides, we carried out GIAO-HF/962+(d) ab initio calculations on various conformers of the known symmetric phosphane selenides **1a** and **1b** and of the new mixed-substituted compounds **1c** and **1d**.[19–22]

Qualitatively, the experimentally observed range of ^{77}Se NMR shieldings (**1c** < **1a** << **1b** < **1d**) reflects fairly well the calculated shift values of their energetically most favourable rotamers (**1cA** < **1a** << **1bA** < **1dA**) (Scheme 2). The range is similar (**1c**, **a** << **1b**, **d**) when the ^{77}Se NMR shifts are averaged according to a Boltzmann

Table 2. ^{31}P NMR shifts [ppm] and coupling constants ^1J (^{77}Se,^{31}P) [Hz] (J values are in italics) of phosphane selenides $R_2R'PSe$ (R, R' = iPr or tBu) **1a**–**d** and of phosphane selenide dibromides **2a**–**d**.

		$R_2R'P$	$R_2R'PSe$ (**1**)		$R_2R'PSeBr_2$ (**2**)	
		δ^{31}P	δ^{31}P	$\lvert ^1J(^{77}\mathrm{Se},^{31}\mathrm{P})\rvert$	δ^{31}P	$\lvert ^1J(^{77}\mathrm{Se},^{31}\mathrm{P})\rvert$
tBu$_3$P	**a**	62.0[a]	93.8[a] 93.3[b]	709[a] 693[b]	83.0[c]	514[c]
tBu$_2$(iPr)P	**c**	46.9[a]	84.6[a] 70.6[b]	706[a] 692[b]	82.9[b]	520[b]
tBu(iPr)$_2$P	**d**	33.3[a]	79.9[a] 84.4[b]	713[a] 688[b]	77.4[b]	526[b]
iPr$_3$P	**b**	19.3[a]	71.1[a] 79.5[b]	709[a] 696[b]	69.8[c]	521[c]

[a] C_6D_6. [b] CD_2Cl_2. [c] CH_2Cl_2/C_6D_6.

Table 3. ^{77}Se NMR shifts [ppm] of phosphane selenides tBu$_n$(iPr)$_{3-n}$PSe.

	n = 3 tBu$_3$PSe **1a**	n = 2 tBu$_2$(iPr)PSe **1c**	n = 1 tBu(iPr)$_2$PSe **1d**	n = 0 iPr$_3$PSe **1b**
	Experimental			
In C_6D_6	–420	–400	–499	–490
In CH_2Cl_2	–417	–394	–493	–482
In CH_3CN	–421	–398	–497	–485
	Calculated (see Scheme 2)			
Most stable rotamer	–427	–408	–567	–480
Second most stable rotamer (E)		–391 (0.5)	–492 (0.3)	–568 (0.7)
Boltzmann-averaged		–403	–500	–519

distribution of the respective rotamers at 298 K (**1c**: –403, **1a**: –427, **1b**: –519, **1d**: –500). Compound **1c**, showing the "abnormally deshielded" ^{77}Se signal (compared with naive expectations from linear interpolation between **1a** and **1b**) is apparently the only compound among the isopropyl derivatives in which no rotamer with *anti* arrangement of the SePCH moiety (which would be **1cC**) contributes to the rotamer-population averaged ^{77}Se NMR shift. Our theoretically determined energies and shifts may still involve significant inaccuracies because of the approximate nature of the methods used.[21,22] Nevertheless, the good qualitative accord between the current computational and experimental results is encouraging. In addition, the MP2/962(d) relative stabilities of rotamers of **1c** correlate fairly well with those calculated previously by an empirical force field (MM2) on the parent phosphane *t*Bu$_2$*i*PrP.[22] It was confirmed by NMR studies on *t*Bu$_2$*i*PrP and its Rh^I and Ir^I complexes that the preferred "GA conformation" (*gauche*/*anti* CH$_3$ groups, corresponding to **1cA/1cB**)[23] of *t*Bu$_2$*i*PrP is essentially retained in its metal complexes.[24,25] Another interesting result from the calculated ^{77}Se NMR shifts is the observation that the shieldings relative to **1a** increase with increasing number of *anti* hydrogen atoms (*anti* arrangement of the SePCH moieties [**1cC** < **1dB** < **1bC**]) and decrease with increasing number of *gauche* hydrogen atoms (**1cA** > **1dC** > **1bD**) in the isopropylphosphorus groups. Direct evidence on these questions can be expected from structure determinations (vide infra) combined with forthcoming solid state ^{77}Se NMR studies.

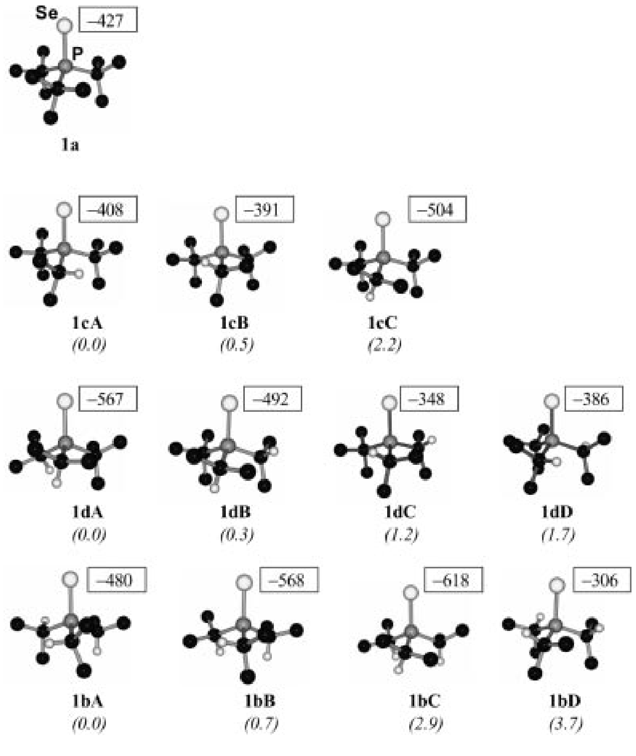

Scheme 2. Optimised rotamer structures of **1a**–**1d** (in italics: MP2-based relative energies [kcal/mol]; in boxes: GIAO-HF computed ^{77}Se chemical shifts).

Structure Determinations

Phosphane Selenide Structures

The molecular structure of *t*Bu$_3$PSe (**1a**) has been determined recently,[26] but the structures of *i*Pr$_3$PSe (**1b**) and of the mixed substituted compounds **1c** and **1d** were not yet known. Differently from **1a**, which displays crystallographic C_3 symmetry implying twisted *tert*-butyl groups,[26] both crystallographically independent molecules of solid **1b** exhibit C_s symmetry (Figure 1). Se,P and the C–H bond of one of the isopropyl groups lie within the mirror plane, and the H–C–P–Se moiety is in a *trans* arrangement. This structure is related to that of the telluride *i*Pr$_3$PTe.[15b] The fact that only one of the C–H bonds of the three isopropyl groups is in a *transoid* arrangement with respect to the PSe bond, and the two other groups display *gauche* type conformations, is in agreement with the calculated *lowest-energy* gas phase structures (**1bA** and **1bB**), but the symmetric orientation of the two twisted isopropyl groups with respect to the mirror plane is not in agreement with calculation. The increase of "1,3 dimethyl strain", also shown by the short contacts H(2A)···H(2A′) 224, H(3C)···H(3C′) 215, H(7A)···H(7A′) 220, H(8C)···H(8C′) 217 pm between the two symmetry-equivalent isopropyl groups in solid **1b**, is reflected by the expanded angle C(1)P(1)C(1′) 112° and C(6)P(1)C(6′) 113° compared with C(1)P(1)C(4) 105° and C(6)P(2)C(9) 105°. The P–C and C–C distances, however, are apparently not affected by this distortion. The related cell constants of **1b** and *i*Pr$_3$PTe (7.630, 11.856, 13.750 Å, β = 100.29°) would suggest some similarity of packing. Figure 2 (a and b) shows the packing projected down the shortest axis in each case. Within the horizontal rows of molecules, the heights are however different; for **1b**, consecutive molecules lie at about 0, ¼, ½, ¼, 0… and for *i*Pr$_3$PTe at 0, ½, 0, ½… (in both cases for the upper row within the cell). One short methine C–H···Se interaction is observed for **1b**, namely H9···Se1 294 pm (within the asymmetric unit).

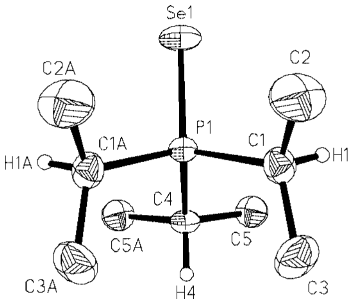

Figure 1. Structure of **1b**, molecule 1 (molecule 2 is very similar), selected bond lengths [pm] and angles [°]: P(1)–Se(1) 212.44(9), C(1)#1–P(1)–C(1) 112.20(15), C(1)#1–P(1)–C(4) 105.56(9), C(1)–P(1)–C(4) 105.56(9). Carbon atoms numbered 6–10 (see text) refer to molecule 2.

Single crystals of suitable quality for structure determinations have not yet been obtained from the mixed-substituted phosphane selenides **1c** and **1d**. A crystalline sample of *t*Bu(*i*Pr)$_2$PSe (**1d**) was investigated, but poor crystal qual-

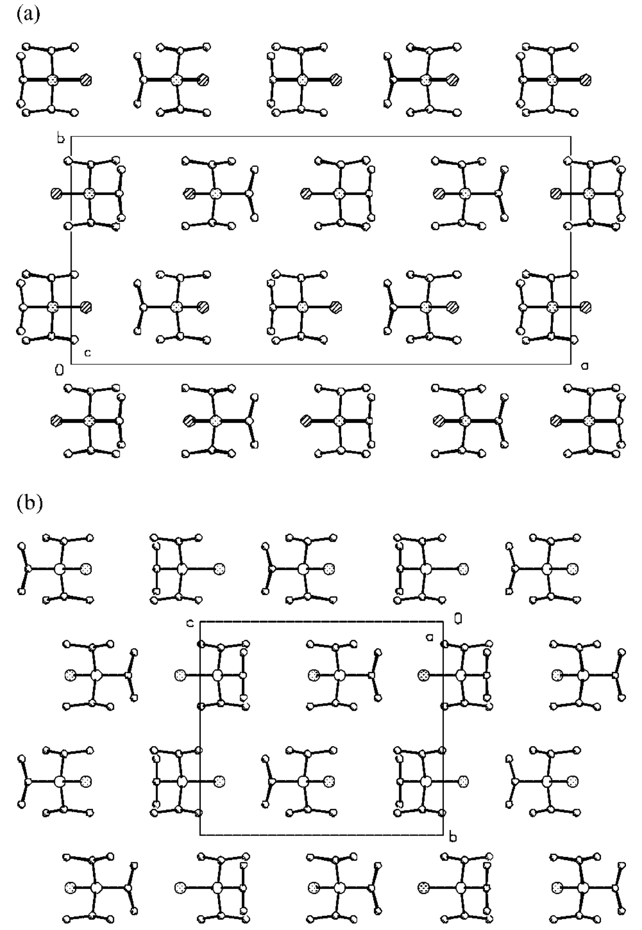

Figure 2. (a) Packing diagram in projection of $i\mathrm{Pr_3PSe}$ (**1b**). (b) Packing diagram in projection of $i\mathrm{Pr_3PTe}$.

ity precluded a satisfactory refinement. The data indicate qualitatively that one of the isopropyl groups adopts a conformation with a *transoid* H–C–P–Se arrangement (as in calcd. structures **1dA**, **1dB**).

The crystalline bromophosphonium salt $t\mathrm{Bu_2}(i\mathrm{Pr})\mathrm{PBr^+Br^-}$ (**3c**) contains a cation that is isoelectronic with **1c**.

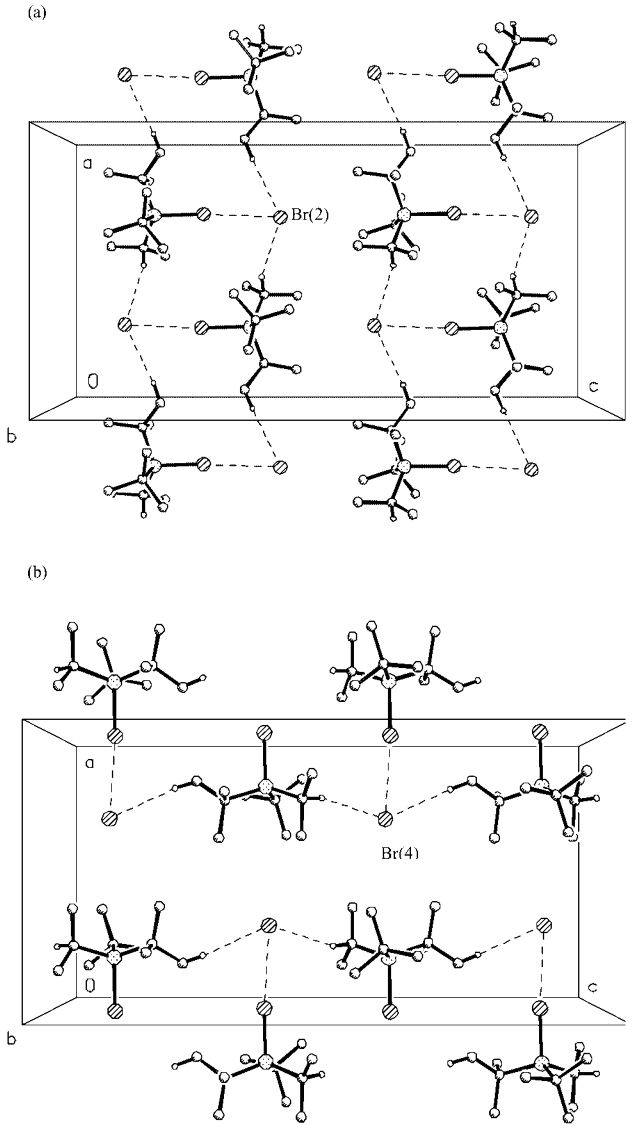

Figure 4. (a) Packing diagrams of the individual formula units of **3c** at $y \cong 0$. (b) Packing diagrams of the individual formula units of **3c** at $y \cong ½$.

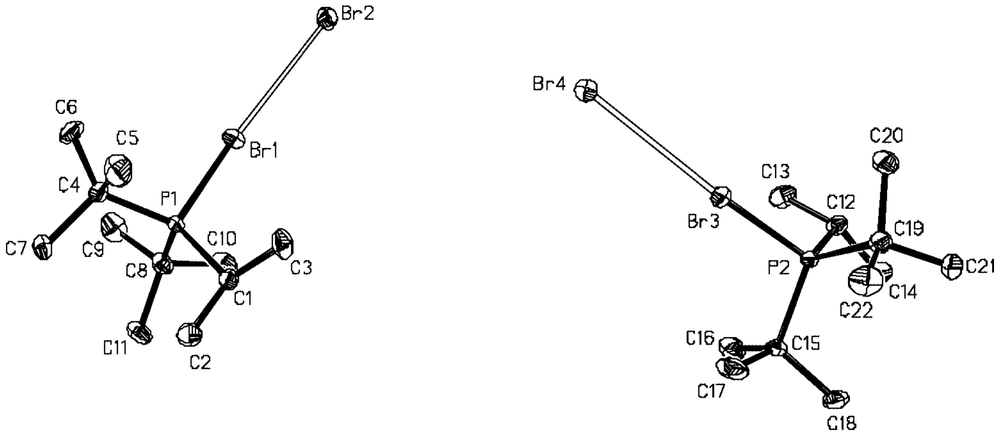

Figure 3. Structure of two ion pairs of **3c**. Selected bond lengths [pm] and angles [°]: P(1)–Br(1) 218.55(7), Br(1)–Br(2) 342.27(4), P(2)–Br(3) 218.62(6), Br(3)–Br(4) 336.79(4), P(1)–Br(1)–Br(2) 175.146(18), P(2)–Br(3)–Br(4) 174.451(18).

Within the asymmetric unit are two independent cation–anion pairs $t\mathrm{Bu}_2(i\mathrm{Pr})\mathrm{PBr}^+$ Br^- (Figure 3). Both pairs display approximately linear P–Br···Br moieties (175.5 ± 1°) with weak ($n \rightarrow \sigma^*$) Br···Br interactions (336.8 and 342.3 pm). Br(1)···Br(2) is roughly parallel to the *c* and Br(3)···Br(4) to the *a* axis. Within both $t\mathrm{Bu}_2(i\mathrm{Pr})\mathrm{PBr}^+$ cations, the H–C–P–Br moiety involving the C–H bond of the isopropyl group is in a *gauche* conformation, as predicted for selenide **1c** (calcd. structures **1cA**, **1cB**) and for the parent phosphane and its Rh and Ir complexes.[24,25] The ion pairs $t\mathrm{Bu}_2(i\mathrm{Pr})\mathrm{PBr}^+$ Br^- exhibit *inter*molecular C–H···Br contacts involving the bromide ions. Considering only contacts H···Br < 300 pm, Br(2) exhibits three and Br(4) four contacts, of which the shortest by far involve the methine protons [C(1)–H(1)···Br(2) 277 pm; C(12)–H(12)···Br(4) 273 pm]. Packing diagrams of the individual formula units (Figure 4, a and b) show that they occupy different regions of the cell at $y \approx 0$ and $y \approx ½$ respectively.

Phosphane Selenide Dibromides

The discussion in the sequence **2b**, **2d**, **2c** follows the increasing steric strain with an increasing number of *tert*-butyl groups in the molecules.

From $i\mathrm{Pr}_3\mathrm{PSeBr}_2$ (**2b**), two different crystalline phases were isolated. The intended preparation of **2b** led by recrystallisation of the crude product from dichloromethane/pentane (vapour diffusion method) to monoclinic crystals ($P2_1/n$, $Z = 4$; **2b**#1). Bromination of **1b** with an excess of bromine led to a mixture of products from which two types of single crystals were collected by crystallisation from dichloromethane: about 50% of a complex material that is apparently $[(i\mathrm{Pr}_3\mathrm{PSeH}^+)_2(i\mathrm{Pr}_3\mathrm{PSeBr}^+)(\mathrm{SeBr}_6{}^{2-})(\mathrm{Se}_2\mathrm{Br}_9)^-]$ (partially disordered),[13b] and a few single crystals of **2b**#2 (monoclinic, $P2_1/n$, $Z = 8$).

All molecules in both phases of **2b** contain $i\mathrm{Pr}_3\mathrm{P}$ coordinated to the central selenium atoms of approximately linear BrSeBr groups (“10-Se-3” according to the J. C. Martin count).[10] The T structures around Se are distorted by unequal Se–Br bond lengths and by PSeBr angles that are larger than 90° (in the opposite sense to the distortion of the “classic” ClF_3 structure). The latter distortion, as in previously known $\mathrm{R}_3\mathrm{PSeBr}_2$ structures, is attributed to steric repulsion between the PR_3 substituent and the bromine atoms.

In the monomeric molecule **2b**#1 (Figure 5, a and b) the BrSeBr group differs from linearity by nearly 13° (angles PSeBr 95.5 and 96.8°) and from Se–Br equidistance by about 12 pm (252.52 and 264.35 pm). The PSe bond length is extended from 212.2 pm (**1b**) to 226.8 pm, which is very similar to that of known $\mathrm{R}_3\mathrm{PSeBr}_2$ structures.[8] The conformation of the $i\mathrm{Pr}_3\mathrm{PSe}$ group differs from that of solid *free* **1b** by lacking the formal mirror plane, but the mirror symmetry is maintained to a good approximation (r.m.s. deviation of molecular halves: 0.08 Å). One of the isopropyl groups adopts a conformation with a *transoid* H–C(1)–P–Se arrangement (as in the calculated structure **1bA**); the other two are twisted, leading to *gauche* type H–C–P–Se conformations. The orientation of the P–C(1) bond is orthogonal to the BrSeBr vector; the approximate mirror symmetry is also shown by the torsion angles [Br(1)SePC(7) –28.46(7)° and Br(2)SePC(4) 29.90(8)°]. As in solid **1b**, CPC angles involving the C atom of the *transoid* HCPSe moiety are significantly smaller (107.8, 108.7°) than that of the two other isopropyl groups [C(4)PC(7) 114.7°]. An explanation for this phenomena is the C–H···Br intramolecular interactions (see below; Figure 6, a). Three short H···Br (296–305 pm) and one short H···Se (3.02 Å) from H(1) link the molecules to form layers parallel to the *ac* plane.

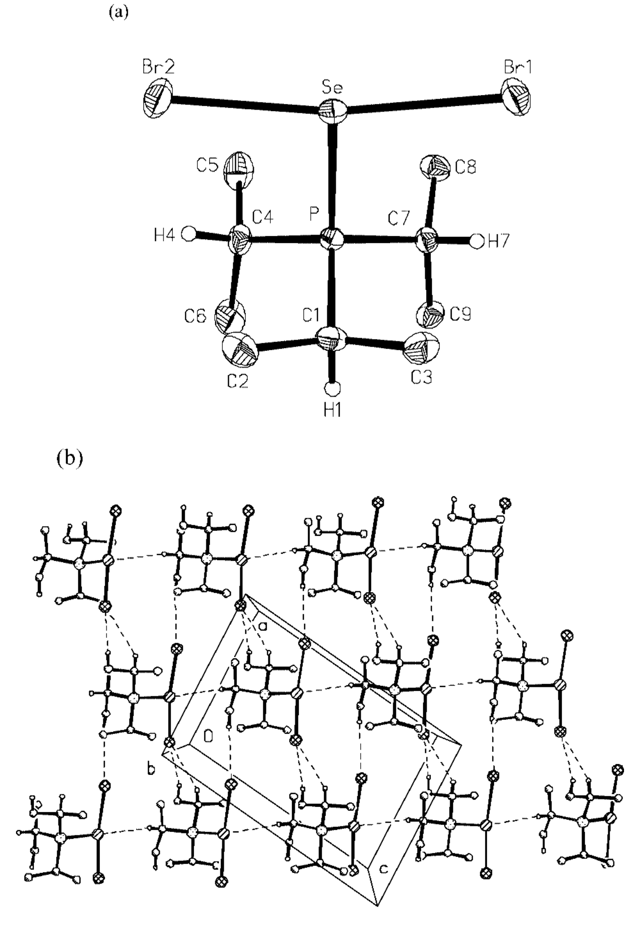

Figure 5. (a) Structure of **2b**#1, $Z = 4$, selected bond lengths [pm] and angles [°]: P–Se 226.81(5), Se–Br(1) 264.35(3), Se–Br(2) 252.52(3), P–Se–Br(1) 96.734(16), P–Se–Br(2) 95.485(16), Br(1)–Se–Br(2) 167.209(11), C(1)–P–C(7) 107.77(10), C(1)–P–C(4) 108.66(10), C(7)–P–C(4) 114.73(10). (b) Intermolecular interactions (CH···Se and CH···Br) in the packing diagram of **2b**#1.

Molecule **2b**#2 (Figure 7, a and b) involves two crystallographically independent molecules that are similar to each other (r.m.s. deviation 0.14 Å) and again display approximate mirror symmetry. The SeBr_2 moieties are more regular than in **2b**#1, with Se···Br 257.56, 260.18 and 254.23, 260.55 pm. In contrast to **2b**#1, which has no significant short contacts of the type Se···Br and Br···Br, there are two such contacts in **2b**#2; Se(1)···Br(3) 346.23(8) within the

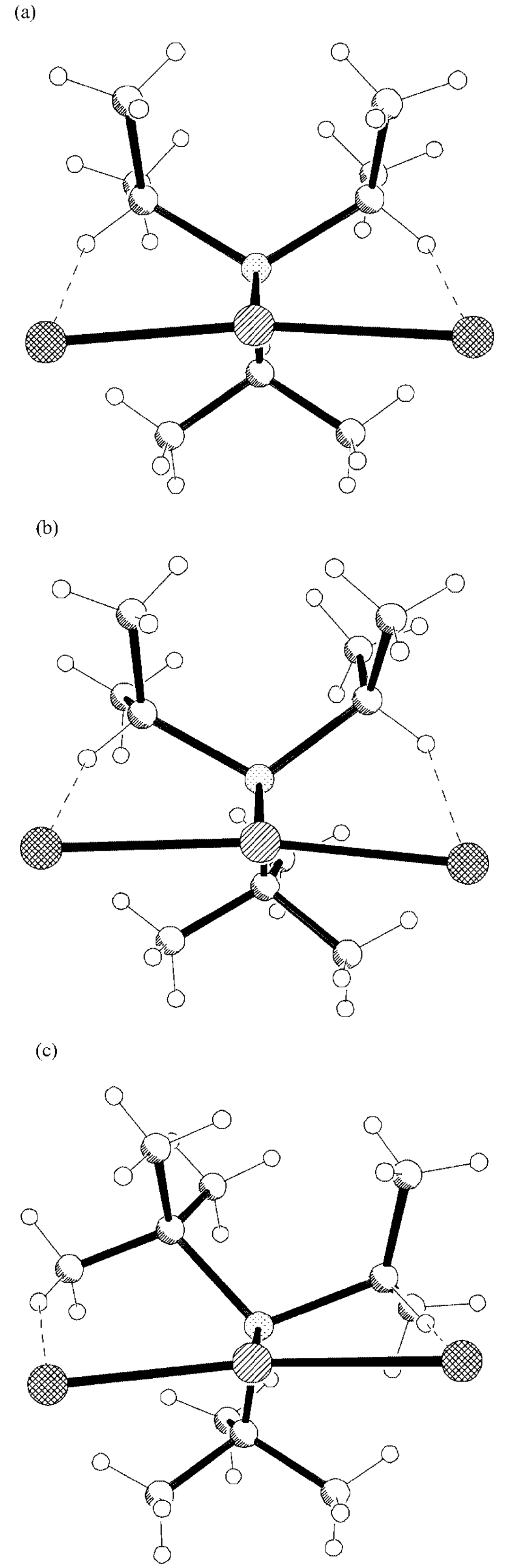

Figure 6. (a) Structure of iPr$_3$PSeBr$_2$, **2b**#1, $Z = 4$; H···Br intramolecular interactions: H(4)···Br(2) 272, H(7)···Br(1) 280 pm. (b) Structure of tBu(iPr)$_2$PSeBr$_2$ (**2d**); H···Br intramolecular interactions: H(5)···Br(1) 299, H(8)···Br(2) 267 pm. (c) Structure of tBu$_2$(iPr)PSeBr$_2$ (**2c**); H···Br intramolecular interactions: H(1)···Br(1) 262, H(9C)···Br(2) 271 pm.

asymmetric unit and Br(4)···Br(4′) 361.22(15) pm. The packing also involves the contact H(1)···Se(2) 303 pm and eight H···Br contacts under 315 pm. The net effect is to form layers parallel to 101.

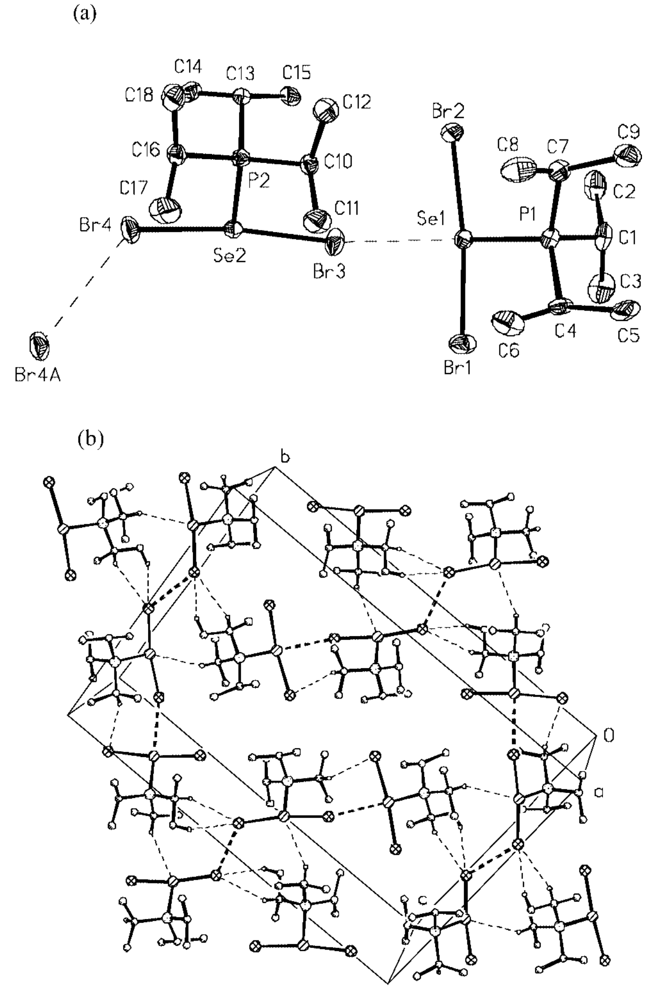

Figure 7. (a) Structure of **2b**#2, $Z = 8$, selected bond lengths [pm] and angles [°]: P(1)–Se(1) 227.34(14), Se(1)–Br(1) 257.56(9), Se(1)–Br(2) 260.18(9), P(1)–Se(1)–Br(1) 94.36(4), P(1)–Se(1)–Br(2) 95.49(4), Br(1)–Se(1)–Br(2) 169.18(3), P(2)–Se(2) 227.15(14), Se(2)–Br(3) 260.55(9), Se(2)–Br(4) 254.23(9), P(2)–Se(2)–Br(3) 96.59(5), P(2)–Se(2)–Br(4) 95.10(5), Br(3)–Se(2)–Br(4) 168.19(3), C(4)–P(1)–C(1) 108.6(3), C(4)–P(1)–C(7) 113.2(2), C(1)–P(1)–C(7) 107.1(3), C(13)–P(2)–C(10) 109.1(3), C(13)–P(2)–C(16) 107.5(3), C(10)–P(2)–C(16) 114.8(2). (b) Intermolecular contacts involving the two types of molecules of **2b**#2.

Formal exchange of one isopropyl group by one *tert*-butyl group in **2b** affords **2d**. Compound **2d** crystallises as centrosymmetric Se–Br···Se-bridged dimers. Two T-shaped PSeBr$_2$ groups associate so that the bridging Br atom of one molecule exhibits contacts to the Se atom (382 pm) and to the bridging Br atom (388 pm) of the neighbouring molecule (Figure 8, a and b). The shorter Se–Br bond is involved in these intermolecular interactions (253.64, cf. 264.95 pm). Compound **2d** deviates significantly from mirror symmetry [e.g. torsion angles C(5)–P–Se–Br(1) –36.9, C(8)–P–Se–Br(2) 24.3°]. The conformation of the *t*Bu(*i*Pr)$_2$PSe group within **2d** differs from that calculated for **2d** in the gas phase. The additional methyl group in **2d** formally replaces the H atom that was part of the *trans*-H–C–P–Se moiety of **2b**; that is, both remaining isopropyl group methine protons are part of *synclinal* H–C–P–Se conformations [H(5)C(5) PSe, $\Theta = 73.3°$; H(8)C(8)PSe, $\Theta = -49°$] (Figure 6, b). Compared with **2b**, the additional methyl group at C(1) [*transoid* C(4)–C(1)–P–Se] enhances the 1,3-dimethyl strain towards C(6) and C(9) of the isopropyl groups leading to approximately equal CPC bond angles (110.6, 111.24, 112.9°), compared with 105/112° in **1b** and 108/115 in **2b**#1. In case of **1d**, such a conformation is expected to be about 1.2 kcal above ground state (**1dC** in Scheme 2). Compounds **2d** and **2b**#1 are not isostructural, despite the similarity of cell constants; **2d** displays four H···Br contacts <315 pm but no H···Se contacts.

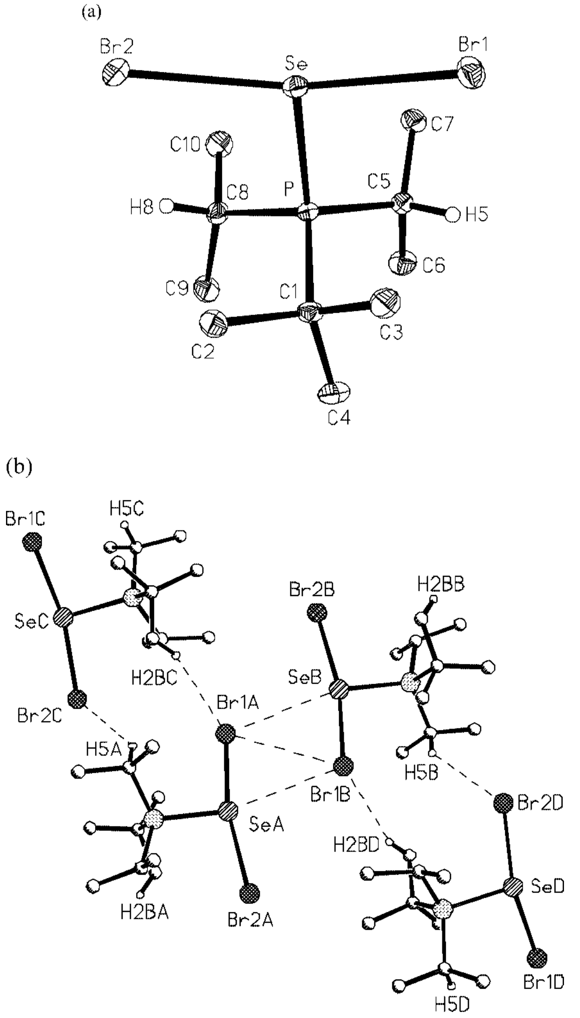

Figure 8. (a) Structure of **2d**, selected bond lengths [pm] and angles [°]: P–Se 228.67(4), Se–Br(1) 253.64(3), Se–Br(2) 264.95(3), P–Se–Br(1) 95.032(12), P–Se–Br(2) 97.462(12), Br(1)–Se–Br(2) 167.104(9), C(8)–P–C(5) 112.93(7), C(8)–P–C(1) 110.60(7), C(5)–P–C(1) 111.24(7). (b) Intermolecular interactions in the packing diagram of **2d**, selected contact distances [pm]: H(5)–Br(2) 305.3, H(2)–Br(1) 298.2, Se–Br(1) 381.68(3), Br(1)–Br(1) 388.02(4).

The structure of *t*Bu$_2$(*i*Pr)PSeBr$_2$ is imprecisely determined for reasons given in the experimental section; the heavy atoms correspond closely to crystallographic mirror (pseudo)symmetry, but the light atoms do not (Figure 9, a). The reason is clearly the intramolecular hydrogen bond H(1)···Br(1) of 262 pm, cf. H(9C)···Br(2) 271 pm, from a methyl hydrogen of a butyl group (Figure 6, c). This leads to torsion angles [°] H(1)–C(1)–P–Se 42, C(1)–P–Se–Br(1) –15.8, cf. C(8)–P–Se–Br(2) 49.2; the bromine Br(1) is thus approximately synperiplanar with the isopropyl carbon C(1). The *tert*-butyl carbon C(6) is antiperiplanar to the selenium, with C(6)–C(4)–P–Se 168.2°.

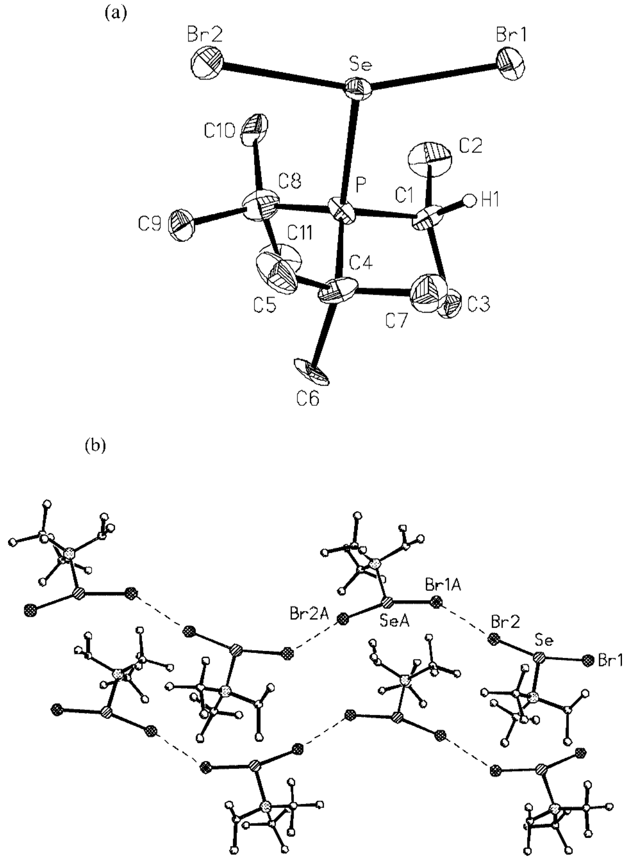

Figure 9. (a) Structure of **2c**, selected bond lengths [pm] and angles [°]: P–Se 230.39(19), Se–Br(1) 262.93(11), Se–Br(2) 255.49(11), P–Se–Br(1) 101.57(6), P–Se–Br(2) 99.22(6), Br(1)–Se–Br(2) 159.16(4), C(4)–P–C(1) 110.6(5), C(4)–P–C(8) 115.2(5), C(1)–P–C(8) 109.0(5). (b) Intermolecular interactions in the packing diagram of **2c**, array of molecules with Br···Br contacts, selected contact distances [pm]: Br(1)–Br(2) 358.90(11).

In view of inaccuracies associated with the pseudosymmetry, it would be unwise to regard light atom bond lengths and angles as reliable in detail. Among the heavy-atom dimensions, Se–Br(1) is appreciably longer than Se–Br(2) [262.93(11), 255.49(11) pm], but the angles BrSeP are almost equal [Br(2)–Se–P 99.22(6)°, Br(1)–Se–P 101.57(6)°], if rather wide.

The PSe bond is longer (230.39 pm) and the deviation of the BrSeBr group from linearity (BrSeBr 159.16°) larger

Table 4. Intramolecular interactions C–H···Br and important torsion angles in solid phosphane selenide dibromides [pm, °].

(**2b**#1) *i*Pr$_3$PSeBr$_2$	H(4)···Br(2)	272	C(4)–P–Se–Br(2)	29.9
	H(7)···Br(1)	280	C(7)–P–Se–Br(1)	–28.5
(**2b**#2) *i*Pr$_3$PSeBr$_2$ (mol1)	H(4)···Br(1)	283	C(4)–P–Se–Br(1)	–33.2
	H(7)···Br(2)	267	C(7)–P–Se–Br(2)	26.8
(**2b**#2) *i*Pr$_3$PSeBr$_2$ (mol2)	H(10)···Br(3)	276	C(10)–P–Se–Br(3)	–28.6
	H(16)···Br(4)	274	C(16)–P–Se–Br(4)	27.4
(**2c**) *t*Bu$_2$*i*PrPSeBr$_2$	H(1)···Br(1)	262	C(1)–P–Se–Br(1)	–15.8
	H(9C)···Br(2)	271	C(8)–P–Se–Br(2)	49.2
(**2d**) *t*Bu*i*Pr$_2$PSeBr$_2$	H(5)···Br(1)	299	C(5)–P–Se–Br(1)	–36.9
	H(8)···Br(2)	267	C(8)–P–Se–Br(2)	24.3

than in any other R$_3$PSeBr$_2$ structure. Intermolecular Br···Br contacts (358.90 pm) between T-shaped moieties of **2c** lead, as in solid *c*-Hex$_3$PSeBr$_2$,[8] to wave-like chains (Figure 9, b) that are packed into layers in the crystal. Additionally, the contact H(7b)···Se 302 pm and four H···Br contacts <315 pm lead to a complex three-dimensional packing.

The observation of the intramolecular C–H···Br interaction in **2c** prompted us to re-assess the other structures; in most cases, the isopropyl C–H groups, the most effective donors available, form a short intramolecular contact to the bromine. Compounds with two such donors thus tend to display exact or approximate mirror symmetry (Figure 6, a and b, Table 4). Hydrogen bonds of the type C–H···halogen have previously been adduced by us as conformation-determining factors.[27]

In summary, steric strain from *tert*-butyl groups correlates with increasing deviation from linearity of the Br–Se–Br groups and with increasing P–Se distances (Table 5). We do not observe, however, a straightforward correlation of intermolecular Se···Br and Br···Br interactions, steric effects and nonequidistance of Se–Br bonds in our series of related trialkylphosphane selenide dibromides. Intramolecular hydrogen bonds of the type C–H···Br determine, to a large extent, the local molecular symmetry.

Table 5. Important bond lengths (P–Se, Se–Br) and intermolecular contacts (Br···Br, Se···Br) in solid phosphane selenide dibromides.

	P–Se	Se–Br	Br···Br	Se···Br
(**1a**) *t*Bu$_3$PSe[25]	213.3	–	–	–
(**1b**) *i*Pr$_3$PSe	212.4	–	–	–
(**2b**) *i*Pr$_3$PSeBr$_2$#1	226.8	252.5, 264.4	–	–
*i*Pr$_3$PSeBr$_2$#2 (mol1)	227.3	257.6, 260.2	361.2	346.2
*i*Pr$_3$PSeBr$_2$#2 (mol2)	227.2	254.2, 260.6	361.2	346.2
(**2c**) *t*Bu$_2$*i*PrPSeBr$_2$	230.4	255.5, 262.9	358.9	–
(**2d**) *t*Bu*i*Pr$_2$PSeBr$_2$	228.7	253.6, 264.9	388.0	381.7

Bromine Exchange Reactions

The NMR phenomena in solutions containing selenides **1** together with the dibromides **2** can be explained by bromine exchange reactions (rapid on the ^{31}P NMR timescale, however in coalescence on the ^{77}Se timescale) that involve Se–Br bond breaking, but do not involve P–Se bond breaking, because $^1J(^{77}\text{Se},^{31}\text{P})$ can be observed at all times from the ^{31}P NMR satellites.

Bromine exchange between selenium atoms has been observed in bromine adducts of bis(arylselanyl)benzenes,[28] but the kinetic lability (bromine exchange) of phosphane chalcogenide dibromides has apparently not yet been recognised in the literature. We suppose that the mode of halogen exchange will be related to that in phosphane–dihalogen equilibrium systems (R$_3$PX$_2$/R$_3$P; X = Br, I).[29] The latter involve nucleophilic attack at halogen atoms in α position (R$_3$PX$^+$←PR$_3$), whereas for the phosphane selenides the same should occur in β position (R$_3$PSeX$^+$←SePR$_3$) from the onium centres. As shown previously, [R$_3$PSeISePR$_3$]$^+$ cations can be stable species in such equilibria.[9] Cations [R$_3$PSeBrSePR$_3$]$^+$, however, have not yet been observed as ground state species.

Support for these interpretations is provided by computations for the model compound Me$_3$PSe and its brominated derivatives. Both types of "1:1 adducts" with Br$_2$ are minima on the potential energy surface, namely the weak donor–acceptor complex **5A** and T-shaped **5B**, the oxidative addition product (Scheme 3). The latter is computed to be more stable than the former by 13.6 kcal/mol and is characterised by a ^{77}Se resonance (δ_{calc} = 454) downfield from that of free Me$_3$PSe. The large stabilisation of **5B** over **5A** is consistent with the exclusive occurrence of type **B** adducts with Br$_2$ (see above). Heterolytical cleavage of **5A** or **5B** into Me$_3$PSeBr$^+$ (**6**) and Br$^-$ is highly unfavourable in the gas phase (109.3 and 123.2 kcal/mol, respectively), but may well be facilitated by polar solvents. The halogen transfer discussed above can proceed via complex **7A**. On the HF/641(d) potential energy surface (PES), **7A**, with its asymmetrical Se–Br···Se arrangement (distances 2.37 and 3.17 Å), is a shallow minimum, about 2 kcal/mol below the C_{2h} symmetric transition state **7B** with equal Se···Br distances (2.65 Å). Inclusion of electron correlation effects by the MP2 single-point energies stabilises **7B**, to 8.7 kcal/mol below the apparent minimum **7A**. It is thus very likely that the symmetrical form is the actual minimum on the true PES (a notion which is supported by an MP2/962+(d) optimisation of **7A**, which afforded symmetrical **7B**); in any event, the proposed halogen transfer reaction by the sequence **7A** $\rightleftharpoons$ **7B** $\rightleftharpoons$ **7A′** (Scheme 3) is indicated to be a facile process.

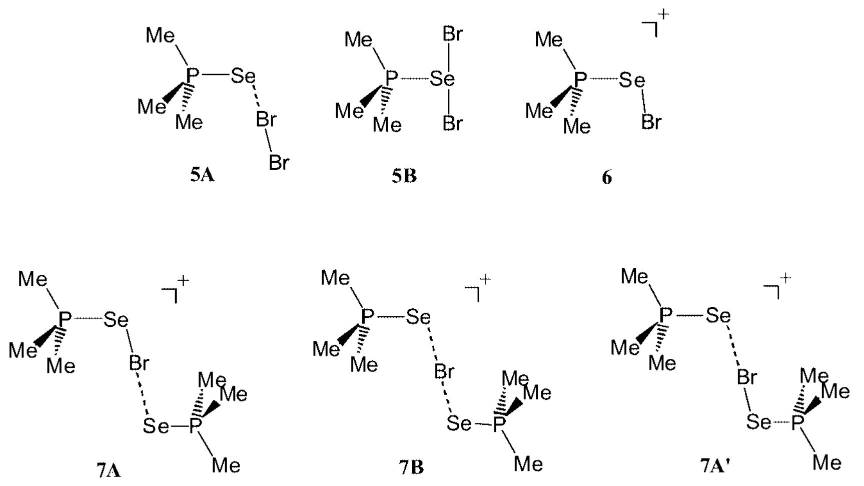

Scheme 3. Bromine transfer between Me_3PSe molecules.

Vibrational Spectra

It is well known that “T-shaped” adducts featuring a linear and symmetric Br–E–Br group (E = S, Se) show in their Raman spectra only one strong peak at around 160 cm^{-1}, because of the symmetric stretching vibration of the Br–E–Br system. A second lower peak at around 190 cm^{-1}, because of the antisymmetric vibration, appears when the Br–E–Br system is asymmetric.[30,31] This vibrational behaviour strictly resembles that observed for $[Br–X–Br]^-$ (X = I, Br) anions,[30,31] which are characterised by a very strong Raman peak at around 160 cm^{-1} accompanied by a weaker one at 190 cm^{-1} when these anions are slightly asymmetric. The FT-Raman spectra of **2b** and **2c** confirm the vibrational analogy between the aforementioned trihalides and the hypervalent Se adducts with Br_2. In fact, they are dominated by very strong peaks, at 169 and 163 cm^{-1} for **2b** and **2c**, respectively, accompanied by weaker peaks at about 190 cm^{-1}, agreeing with the slight asymmetry of the Br–Se–Br groups observed for the two compounds by X-ray analysis. The Raman spectrum of **2d** also shows a peak at 163.9 cm^{-1} accompanied by a weaker one at 190 cm^{-1} with the difference that compared to **2b** and **2c** the intensity of the peak at 163.9 is much lower. In the FTIR spectra of **2b** and **2c** two broad bands at about the same frequencies of those observed in the Raman spectra are present with an increased intensity for the band because of the antisymmetric stretching of the Br–Se–Br group. For **2d**, the quality of the FTIR spectra does not provide any additional information.

The Raman spectrum of the ionic pair **3c** show a very weak peak at 180 cm^{-1}, which cannot be attributable to a Br–Br stretching vibration, the Br···Br distance being very long. Therefore, we think that this peak might be originated by vibration modes involving the P–Br bond and the remaining organic framework of the cation in the ionic pair.

Discussion

GIAO-HF/962+(d) calculations on the ^{77}Se NMR shifts of related trialkylphosphane selenides **2a–d** allow an explanation of the differences between their ^{77}Se NMR shifts on the basis of particular conformations of their Se–P–C–H groups. The surprising ^{125}Te deshielding of *t*Bu_3PTe relative to *i*Pr_3PTe[15] can be explained in a similar way.

All known phosphane selenide dibromides contain three-coordinate selenium in distorted T-shaped environments. Similar to related bromine adducts from precursors with C=Se bonds,[30] solid phosphane selenide dibromides tend to exhibit intermolecular Se···Br and/or Br···Br “*soft–soft interactions*”. Small variations in the alkyl groups at phosphorus lead to large differences in the pattern of intermolecular contacts. In solution, phosphane selenide dibromides **2a–d** are kinetically labile with respect to reversible bromine transfer to their parent phosphane selenides (averaged ^{1}H, ^{13}C and ^{31}P NMR signals, coalescing ^{77}Se signals in R_3PSeBr_2/R_3PSe mixtures). Calculations show that nucleophilic attack of R_3PSe at the Br atom of a R_3PSeBr^+ cation (Br^+ transfer) is a low-energy pathway for bromine exchange. ^{77}Se NMR signals of pure compounds R_3PSeBr_2 appear about 900–1000 ppm downfield from R_3PSe, and their $^{1}J(^{77}Se,^{31}P)$ coupling constants are 30% smaller than those of R_3PSe. Addition of electrophiles to dissolved compounds R_3PSeBr_2 led to a further decrease of $^{1}J(^{77}Se,^{31}P)$ to less than 500 Hz, but isolation of salts with R_3PSeBr^+ cations was not achieved.

Experimental Section

NMR Spectra: NMR spectra were recorded using Bruker spectrometers AC 200, Avance 200, Avance 400 and AMX 300, with 85% H_3PO_4, $(CH_3)_2Se$ and $SiMe_4$ as external or internal standards. For the measurements of **1a–d** compounds we used 10% solution of $(CH_3)_2Se$ in C_6D_6 and CD_2Cl_2 as standards.

FT-Raman Spectra: FT-Raman spectra in the range 500–50 cm^{-1} were recorded with a resolution of 2 cm^{-1} on a Bruker RFS100 FT-Raman spectrometer, fitted with an In-Ga-As detector (room temperature) operating with a Nd-YAG laser (excitation wavelength 1064 nm; 100 mW), with a 180° scattering geometry. Infrared spectra were recorded with a Bruker IFS55 spectrometer at room temperature, purging the sample cell with a flow of dried air.

Polythene pellets with a mylar beam-splitter and polythene windows (500–50 cm^{-1}, resolution 2 cm^{-1}) were used.

2a: Bromine (330 mg, 2.1 mmol) was added slowly through a dropping funnel to a solution of *t*Bu$_3$PSe (**1b**) (590 mg, 2.1 mmol) in dichloromethane (10 mL) in a Schlenk tube. The red-orange solution was stirred for a further 2 h at room temperature, whereafter the crude product **2a** was isolated by vacuum evaporation of the solvent and purified by washing with pentane, drying by vacuum evaporation. Yield: approx. 89%; m.p. 92 °C; elemental analysis: C$_{12}$H$_{27}$Br$_2$PSe (281.28): calcd. C 32.68, H 6.17; found C 30.62, H 5.94. MS (FAB, *o*-nitrobenzylamine matrix): *m*/*z*, pos. (%) = 57 [100, (*t*Bu)$^+$], 361 [78, (*t*Bu$_3$PSeBr)$^+$], 226 [17, (*t*Bu$_2$PSe)$^+$], 282 [33, (*t*Bu$_3$PSe)$^+$], 305 [31, (*t*Bu$_2$PSeBr)$^+$], 169 [28, (*t*BuPSe)$^+$], 89 [25, (*t*BuP)$^+$]; *m*/*z*, neg. (%) = 294 [100, {(NBA – NH$_2$) + SeBr}$^-$], 375 [85, {(NBA – NH$_2$) + SeBr$_2$}$^-$], 234 [36, (NBA + Br)$^-$], 79 [34, (Br)$^-$]; EI-MS: *m*/*z* (%) = 57 [100, (*t*Bu)$^+$], 170 [43, (*t*BuPSe)$^+$], 282 [17, (*t*Bu$_3$PSe)$^+$], 226 [17, (*t*Bu$_2$PSe)$^+$], 160 [10, (Br$_2$)$^+$], 111 [3, (PSe)$^+$]. ^{31}P NMR (CH$_2$Cl$_2$/C$_6$D$_6$): δ = 83.0 (s, $^1J_{\mathrm{P,Se}}$ = 514 Hz) ppm.

2b: Bromine (330 mg, 2.1 mmol) was added slowly through a dropping funnel to a solution of *i*Pr$_3$PSe (**1b**) (500 mg, 2.1 mmol) in dichloromethane (10 mL) in a Schlenk tube. The red-orange solution was stirred for a further 60 min at room temperature, whereafter the crude product **2b** was isolated by vacuum evaporation of the solvent and purified by washing with pentane, drying by vacuum evaporation and recrystallised by gas diffusion from dichloromethane/pentane. Yield: approx. 78%; m.p. 72 °C; elemental analysis: C$_9$H$_{21}$Br$_2$PSe (239.20): calcd. C 27.09, H 5.30; found C 27.04, H 5.32. MS (FAB, *o*-nitrobenzylamine matrix): *m*/*z*, pos. (%) = 177 [100, (*i*Pr$_3$POH)$^+$], 319 [47, (*i*Pr$_3$PSeBr)$^+$], 353 [32, (*i*Pr$_3$PO)$_2$H$^+$], 240 [8, (*i*Pr$_3$PBr)$^+$]; *m*/*z*, neg. (%) = 232 [77, (NBA·Br)$^-$], 79 [45, (Br)$^-$]; EI-MS: *m*/*z* (%) = 160 [100, (Br$_2$)$^+$], 79 [10, (Br)$^+$], 240 [2, (*i*Pr$_3$PSe)$^+$], 43 [2, (*i*Pr)$^+$]. IR (50–500 cm^{-1}): 93 (s), 119 (m), 143 (s), 172 (s), 186 (s), 279 (vw), 340 (w), 417 (m), 433 (m); Raman (500–50 cm^{-1}): 418 (vw), 385 (vw), 270 (vw), 187 (m), 169 (vs), 145 (m), 94 (m). ^{31}P NMR (CH$_2$Cl$_2$/C$_6$D$_6$): δ = 69.8 (s, $^1J_{\mathrm{P,Se}}$ = 521 Hz) ppm. ^{77}Se NMR (CH$_2$Cl$_2$/C$_6$D$_6$): δ = 409.0 (d, $^1J_{\mathrm{P,Se}}$ = 521 Hz) ppm.

2c: Di-*tert*-butylisopropylphosphane selenide (0.82 g, 3.07 mmol) was dissolved in dichloromethane (40 mL) and a solution of bromine (0.50 g, 3.07 mmol) in dichloromethane (40 mL) was added. The reaction mixture was stirred at room temperature for one day. Solvent was removed in vacuo and the powdery bright orange (di-*tert*-butylisopropylphosphane selenide)–Br$_2$ complex was obtained. Yield: 1.24 g (94%); m.p. 111 °C; elemental analysis: C$_{11}$H$_{25}$Br$_2$PSe (267.25): calcd. C 30.94, H 5.90; found: C 28.64, H 5.64. MS (FAB, *o*-nitrobenzylamine matrix): *m*/*z*, pos. (%) = 77 [100, (C$_6$H$_5$)$^+$ or (C$_3$H$_{10}$P)$^+$], 57 [88, (*t*Bu)$^+$], 136 [65, (NBA – OH)$^+$], 107 [61, (NBA – CH$_2$OH – O)$^+$], 189 [30, (*t*Bu$_2$*i*PrP + H)$^+$], 154 [28, (NBA + H)$^+$], 269 [25, (*t*Bu$_2$*i*PrPSe + H)$^+$], 212 [23, (*t*Bu*i*PrPSe + H)$^+$]; *m*/*z*, neg. (%) = 232 [100, (NBA+Br)$^-$], 153 [88, (NBA)$^-$], 81 [50, (Br)$^-$], 168 [49, (NBA + CH$_3$)$^-$], 122 [41, (NBA + H$_2$O)$^-$], 305 [35, (2NBA – H)$^-$]; EI-MS: *m*/*z* (%) = 268 [100, (*t*Bu$_2$*i*PrPSe)$^+$], 57 [95, (*t*Bu)$^+$], 156 [76, (*i*PrPSe + 2H)$^+$], 212 [40, (*t*Bu*i*PrPSe + H)$^+$], 160 [31, (Br$_2$)$^+$], 43 [10, (*i*Pr)$^+$], 81 [5, (Br)$^+$]. ^{1}H NMR (CD$_2$Cl$_2$): δ = 3.97 [m, C*H*(CH$_3$)$_2$], 1.76 [d, $^3J_{\mathrm{H,P}}$ = 16.7 Hz, C(C*H*$_3$)$_3$], 1.67 [dd, $^3J_{\mathrm{H,H}}$ = 7.3, $^3J_{\mathrm{H,P}}$ = 16.4 Hz, CH(C*H*$_3$)$_2$] ppm. ^{13}C NMR (CD$_2$Cl$_2$): δ = 44.5 [d, $^1J_{\mathrm{C,P}}$ = 13.2 Hz, *C*(CH$_3$)$_3$], 31.8 [d, $^1J_{\mathrm{C,P}}$ = 18.5 Hz, *C*H(CH$_3$)$_2$], 30.1 [s, C(*C*H$_3$)$_3$], 21.1 [d, $^2J_{\mathrm{C,P}}$ = 3.5 Hz, CH(*C*H$_3$)$_2$] ppm. ^{31}P NMR (CD$_2$Cl$_2$): δ = 82.9 (s, $^1J_{\mathrm{P,Se}}$ = 520.2 Hz) ppm.

2d: *tert*-Butyldiisopropylphosphane selenide (0.50 g, 1.97 mmol) was dissolved in dichloromethane (30 mL) and a solution of bromine (0.31 g, 1.97 mmol) in dichloromethane (30 mL) was added. The reaction mixture was stirred at room temperature for one day. The solvent was removed in vacuo and the solid orange (*tert*-butyldiisopropylphosphane selenide)–Br$_2$ complex was obtained. Yield: 0.76 g (93.39%); m.p. 74 °C; elemental analysis: C$_{10}$H$_{23}$Br$_2$PSe (253.23): calcd. C 29.08, H 5.61; found C 29.32, H 5.66. MS (FAB, *o*-nitrobenzylamine matrix): *m*/*z*, pos. (%) = 57 [100, (*t*Bu)$^+$], 333 [90, (*t*Bu*i*Pr$_2$PSeBr)$^+$], 154 [70, (NBA + H)$^+$], 191 [65, (*t*Bu*i*Pr$_2$POH)$^+$], 136 [60, (NBA – OH)$^+$], 255 [38, (*t*Bu*i*Pr$_2$PSe)$^+$], 307 [15, (2NBA + H)$^+$], 413 [4, (*t*Bu*i*Pr$_2$PSeBr$_2$)$^+$]; *m*/*z*, neg. (%) = 153 [100, (NBA)$^-$], 232 [95, (NBA + Br)$^-$], 306 [75, (2NBA)$^-$], 168 [42, (NBA + CH$_3$)$^-$], 122 [22, (NBA + H$_2$O)$^-$], 79 [18, (Br)$^-$], 414 [6, (*t*Bu*i*Pr$_2$PSeBr$_2$)$^-$]; EI-MS: *m*/*z* (%) = 156 [100, (*i*PrPSe + 2 H)$^+$], 57 [95, (*t*Bu)$^+$], 254 [50, (*t*Bu*i*Pr$_2$PSe)$^+$], 198 [40, (*i*Pr$_2$PSe + H)$^+$], 111 [12, (PSe)$^+$], 80 [10, (Br)$^+$]. ^{1}H NMR (CD$_2$Cl$_2$): δ = 3.48 [m, C*H*(CH$_3$)$_2$], 1.55 [dd, $^3J_{\mathrm{H,H}}$ = 6.6, $^3J_{\mathrm{H,P}}$ = 16.9 Hz, CH(C*H*$_3$)$_2$], 1.52 [d, $^3J_{\mathrm{H,P}}$ = 16.6 Hz, C(C*H*$_3$)$_3$] ppm. ^{13}C NMR (CD$_2$Cl$_2$): δ = 28.6 [d, $^1J_{\mathrm{C,P}}$ = 26.3 Hz, *C*(CH$_3$)$_3$], 25.9 [d, $^1J_{\mathrm{C,P}}$ = 26.4 Hz, *C*H(CH$_3$)$_2$], 24.8 [s, C(*C*H$_3$)$_3$], 19.8 [d, $^2J_{\mathrm{C,P}}$ = 3.5 Hz, CH(*C*H$_3$)$_2$], 17.5 [d, $^2J_{\mathrm{C,P}}$ = 3.1 Hz, CH(*C*H$_3$)$_2$] ppm. ^{31}P NMR (CD$_2$Cl$_2$): δ = 77.4 (s, $^1J_{\mathrm{P,Se}}$ = 526.2 Hz) ppm. ^{77}Se NMR (CDCl$_3$): δ = 537.0 (d, $^1J_{\mathrm{Se,P}}$ = 521.6 Hz) ppm.

1a^1: ^{1}H NMR (C$_6$D$_6$): δ = 1.32 [d, $^3J_{\mathrm{H,P}}$ = 13.9 Hz, C(C*H*$_3$)$_3$] ppm. ^{13}C NMR (C$_6$D$_6$): δ = 40.9 [d, $^1J_{\mathrm{C,P}}$ = 26.4 Hz, *C*(CH$_3$)$_3$], 30.5 [s, *C*H(CH$_3$)$_2$] ppm. ^{31}P NMR (C$_6$D$_6$): δ = 93.8 (s, $^1J_{\mathrm{P,Se}}$ = 708.5 Hz) ppm. ^{77}Se NMR (C$_6$D$_6$): δ = –420.3 (d, $^1J_{\mathrm{Se,P}}$ = 707.0 Hz) ppm.

1a^2: ^{1}H NMR (CD$_2$Cl$_2$): δ = 1.41 [d, $^3J_{\mathrm{H,P}}$ = 14.2 Hz, C(C*H*$_3$)$_3$] ppm. ^{13}C NMR (CD$_2$Cl$_2$): δ = 41.0 [d, $^1J_{\mathrm{C,P}}$ = 26.2 Hz, *C*(CH$_3$)$_3$], 30.5 [s, *C*H(CH$_3$)$_2$] ppm. ^{31}P NMR (CD$_2$Cl$_2$): δ = 93.3 (s, $^1J_{\mathrm{P,Se}}$ = 692.9 Hz) ppm. ^{77}Se NMR (CD$_2$Cl$_2$): δ = –417.0 (d, $^1J_{\mathrm{Se,P}}$ = 692.8 Hz) ppm.

1b^1: ^{1}H NMR (C$_6$D$_6$): δ = 1.89 [m, $^3J_{\mathrm{H,H}}$ = 7.0, $^2J_{\mathrm{H,P}}$ = 10.0 Hz, C*H*(CH$_3$)$_2$], 1.03 [dd, $^3J_{\mathrm{H,H}}$ = 7.1, $^3J_{\mathrm{H,P}}$ = 16.0 Hz, CH(C*H*$_3$)$_2$] ppm. ^{13}C NMR (C$_6$D$_6$): δ = 26.8 [d, $^1J_{\mathrm{C,P}}$ = 38.7 Hz, *C*H(CH$_3$)$_2$], 18.2 [d, $^2J_{\mathrm{C,P}}$ = 2.1 Hz, CH(*C*H$_3$)$_2$] ppm. ^{31}P NMR (C$_6$D$_6$): δ = 71.1 (s, $^1J_{\mathrm{P,Se}}$ = 709.2 Hz) ppm. ^{77}Se NMR (C$_6$D$_6$): δ = –489.9 (d, $^1J_{\mathrm{Se,P}}$ = 707.9 Hz) ppm.

1b^2: ^{1}H NMR (CD$_2$Cl$_2$): δ = 2.17 [m, $^3J_{\mathrm{H,H}}$ = 7.1, $^2J_{\mathrm{H,P}}$ = 10.1 Hz, C*H*(CH$_3$)$_2$], 1.16 [dd, $^3J_{\mathrm{H,H}}$ = 7.1, $^3J_{\mathrm{H,P}}$ = 16.2 Hz, CH(C*H*$_3$)$_2$] ppm. ^{13}C NMR (CD$_2$Cl$_2$): δ = 26.8 [d, $^1J_{\mathrm{C,P}}$ = 38.6 Hz, *C*H(CH$_3$)$_2$], 18.0 [d, $^2J_{\mathrm{C,P}}$ = 2.2 Hz, CH(*C*H$_3$)$_2$] ppm. ^{31}P NMR (CD$_2$Cl$_2$): δ = 70.6 (s, $^1J_{\mathrm{P,Se}}$ = 691.9 Hz) ppm. ^{77}Se NMR (CD$_2$Cl$_2$): δ = –481.5 (d, $^1J_{\mathrm{Se,P}}$ = 692.8 Hz) ppm.

1c^1: ^{1}H NMR (C$_6$D$_6$): δ = 2.06 [m, $^3J_{\mathrm{H,H}}$ = 7.3, $^2J_{\mathrm{H,P}}$ = 11.9 Hz, C*H*(CH$_3$)$_2$], 1.29 [dd, $^3J_{\mathrm{H,H}}$ = 7.3, $^3J_{\mathrm{H,P}}$ = 14.9 Hz, CH(C*H*$_3$)$_2$], 1.24 [d, $^3J_{\mathrm{H,P}}$ = 14.2 Hz, C(C*H*$_3$)$_3$] ppm. ^{13}C NMR (C$_6$D$_6$): δ = 38.6 [d, $^1J_{\mathrm{C,P}}$ = 30.1 Hz, *C*(CH$_3$)$_3$], 30.7 [d, $^1J_{\mathrm{C,P}}$ = 31.6 Hz, *C*H(CH$_3$)$_2$], 29.2 [d, $^2J_{\mathrm{C,P}}$ = 1.0 Hz, C(*C*H$_3$)$_3$], 21.4 [d, $^2J_{\mathrm{C,P}}$ = 2.7 Hz, CH(*C*H$_3$)$_2$] ppm. ^{31}P NMR (C$_6$D$_6$): δ = 84.6 (s, $^1J_{\mathrm{P,Se}}$ = 706.2 Hz) ppm. ^{77}Se NMR (C$_6$D$_6$): δ = –399.8 (d, $^1J_{\mathrm{Se,P}}$ = 705.8 Hz) ppm.

1c^2: ^{1}H NMR (CD$_2$Cl$_2$): δ = 2.26 [m, $^3J_{\mathrm{H,H}}$ = 7.3, $^2J_{\mathrm{H,P}}$ = 12.2 Hz, C*H*(CH$_3$)$_2$], δ = 1.45 [dd, $^3J_{\mathrm{H,H}}$ = 7.3, $^3J_{\mathrm{H,P}}$ = 15.6 Hz, CH(C*H*$_3$)$_2$], 1.34 [d, $^3J_{\mathrm{H,P}}$ = 14.4 Hz, C(C*H*$_3$)$_3$] ppm. ^{13}C NMR (CD$_2$Cl$_2$): δ = 38.8 [d, $^1J_{\mathrm{C,P}}$ = 29.8 Hz, *C*(CH$_3$)$_3$], 31.0 [d, $^1J_{\mathrm{C,P}}$ = 31.7 Hz, *C*H(CH$_3$)$_2$], 29.2 [d, $^2J_{\mathrm{C,P}}$ = 0.5 Hz, C(*C*H$_3$)$_3$], 21.4 [d, $^2J_{\mathrm{C,P}}$ = 2.9 Hz, CH(*C*H$_3$)$_2$] ppm. ^{31}P NMR (CD$_2$Cl$_2$): δ = 84.4 (s, $^1J_{\mathrm{P,Se}}$ = 687.7 Hz) ppm. ^{77}Se NMR (CD$_2$Cl$_2$): δ = –393.8 (d, $^1J_{\mathrm{Se,P}}$ = 688.2 Hz) ppm.

1d^1: ^{1}H NMR (C$_6$D$_6$): δ = 2.0 [m, $^3J_{\mathrm{H,H}}$ = 7.0, $^2J_{\mathrm{H,P}}$ = 9.1 Hz, C*H*(CH$_3$)$_2$], 1.10 [d,d, $^4J_{\mathrm{H,H}}$ = 0.2, $^3J_{\mathrm{H,P}}$ = 14.5 Hz, C(C*H*$_3$)$_3$], 1.09 [dd, $^3J_{\mathrm{H,H}}$ = 7.1, $^3J_{\mathrm{H,P}}$ = 15.7 Hz, CH(C*H*$_3$)$_2$], 1.07 [dd, $^3J_{\mathrm{H,H}}$ =

7.0, ${}^3J_{H,P}$ = 15.4 Hz, CH(CH_3)$_2$] ppm. ^{13}C NMR (C_6D_6): δ = 35.3 [d, ${}^1J_{C,P}$ = 34.3 Hz, C(CH$_3$)$_3$], 28.2 [d, ${}^2J_{C,P}$ = 0.9 Hz, C(CH$_3$)$_3$], 26.6 [d, ${}^1J_{C,P}$ = 36.3 Hz, CH(CH$_3$)$_2$], 19.5 [d, ${}^2J_{C,P}$ = 1.9 Hz, CH(CH$_3$)$_2$], δ = 18.8 [d, ${}^2J_{C,P}$ = 2.1 Hz, CH(CH$_3$)$_2$] ppm. ^{31}P NMR (C_6D_6): δ = 79.9 (s, ${}^1J_{P,Se}$ = 712.7 Hz) ppm. ^{77}Se NMR (C_6D_6): δ = –499.2 (d, ${}^1J_{Se,P}$ = 711.5 Hz) ppm.

1d^2: ^{1}H NMR (CD_2Cl_2): δ = 2.3 [m, ${}^3J_{H,H}$ = 7.0, ${}^2J_{H,P}$ = 9.1 Hz, CH(CH$_3$)$_2$], 1.22 [d,d, ${}^4J_{H,H}$ = 0.4, ${}^3J_{H,P}$ = 14.6 Hz, C(CH_3)$_3$], 1.21 [dd, ${}^3J_{H,H}$ = 6.9, ${}^3J_{H,P}$ = 15.9 Hz, CH(CH_3)$_2$], 1.19 [dd, ${}^3J_{H,H}$ = 7.0, ${}^3J_{H,P}$ = 15.5 Hz, CH(CH_3)$_2$] ppm. ^{13}C NMR (CD_2Cl_2): δ = 35.5 [d, ${}^1J_{C,P}$ = 34.1 Hz, C(CH$_3$)$_3$], 28.2 [s, C(CH$_3$)$_3$], 26.7 [d, ${}^1J_{C,P}$ = 36.3 Hz, CH(CH$_3$)$_2$], 19.4 [d, ${}^2J_{C,P}$ = 2.0 Hz, CH(CH$_3$)$_2$], 18.4 [d, ${}^2J_{C,P}$ = 2.2 Hz, CH(CH$_3$)$_2$] ppm. ^{31}P NMR (CD_2Cl_2): δ = 79.5 (s, ${}^1J_{P,Se}$ = 695.8 Hz) ppm. ^{77}Se NMR (CD_2Cl_2): δ = –493.2 (d, ${}^1J_{Se,P}$ = 694.8 Hz) ppm.

Computational Details: The same methods and basis sets as in two former computational studies on ^{77}Se chemical shifts were employed.[19] Specifically, geometries were fully optimised at the restricted Hartree–Fock (HF) level employing the 641(d) basis set, that is, Binning and Curtiss' contracted [6s4p1d] basis on Se and Br,[19a] a contracted [2s] double-zeta Huzinaga basis on H (DZ),[20b] and standard 6-31G* basis on P and C.[20c,20d] All minima were characterised as such by computation of the harmonic vibrational frequencies. Single-point energy calculations for these geometries were performed at the electron-correlated second-order Møller–Plesset (MP2) level using the larger 962(d) basis, that is, a decontracted version of the 641(d) basis on Se and Br,[20a] DZ basis on H, Dunning's polarised (α_d = 0.75) [5s3p] basis on C,[20e] and McLean and Chandler's polarised (α_d = 0.465) [6s5p] basis on P.[20f] Relative energies are reported at the MP2/962(d)//HF/641(d) level (in the "level of energy evaluation // level of geometry optimisation" notation), corrected for the HF/641(d) zero-point energies (scaled by 0.9).

Magnetic shieldings were computed at the HF level with the Gauge-Including-Atomic-Orbitals (GIAO) method, as implemented[21] in the Gaussian 98 program,[22] employing the HF/641(d) geometries and 962+(d) basis, that is, the same as 962(d), but augmented with a set of diffuse s and p functions on Se (α_s = α_p = 0.022),[20a] which were shown to be beneficial in many cases.[19a] δ^{77}Se chemical shifts are reported relative to Me$_2$Se, the experimental standard, for which an absolute shielding constant of 1905 ppm is obtained at the same level.

X-ray Structure Determinations: Numerical details are presented in Table 6. *Data collection and reduction*: Crystals were mounted in inert oil on glass fibres and transferred to the cold gas stream of the diffractometer (**1b**: Stoe STADI-4; **2b**#2, **2c**: Siemens P4; **2b**#1, **2d**, **3c**: Bruker SMART 1000 CCD). Measurements were performed with monochromated Mo-K_α radiation. Absorption corrections for the area detector were performed with the program SADABS, and for the serial diffractometers on the basis of ψ-scans. The crystal of **2c** decomposed appreciably even at low temperature and data were scaled accordingly. *Structure solution and refinement*: The structures were refined anisotropically against F^2 (program SHELXL-97, G.M. Sheldrick, University of Göttingen). H atoms were included with a riding model or as rigid methyl groups. *Special features of refinement*: Compound **2c** was refined as an enantiomeric twin, with Flack parameter 0.46(3); it is severely pseudosymmetric, with P, Se and Br atoms lying in a pseudomirror plane corresponding to the higher symmetry space group *Pnma*, but the alkyl groups clearly rotated out of the mirror-symmetric positions. Methyl hydrogens were placed in ideally staggered positions. Despite the use of distance restraints, the light atom bond lengths and angles were distorted and of limited reliability. CCDC-282196 (for **1b**), -282197 (for **2b**#1), -282198 (for **2b**#2), -282199 (for **2c**), -282200 (for **2d**) and -282201 (for **3c**) contain the supplementary crystallographic data for this paper. These data can

Table 6. Crystallographic data.

	1b	**2b**#1	**2b**#2	**2c**	**2d**	**3c**
Formula	$C_9H_{21}PSe$	$C_9H_{21}Br_2PSe$	$C_9H_{21}Br_2PSe$	$C_{11}H_{25}Br_2PSe$	$C_{10}H_{23}Br_2PSe$	$C_{11}H_{25}Br_2P$
M_r	239.19	399.01	399.01	427.06	413.03	348.10
Habit	colourless prism	pale orange prism	yellow tablet	red tablet	red tablet	red tablet
Crystal size [mm]	0.6×0.6×0.5	0.27×0.2×0.13	0.6×0.5×0.18	0.4×0.3×0.2	0.45×0.3×0.3	0.3×0.2×0.1
Crystal system	orthorhombic	monoclinic	monoclinic	orthorhombic	monoclinic	monoclinic
Space group	*Pnma*	$P2_1/n$	$P2_1/n$	$Pna2_1$	$P2_1/n$	$P2/c$
a [pm]	2619.0(5)	838.65(6)	750.38(10)	1586.82(15)	755.56(6)	1111.95(8)
b [pm]	1193.13(14)	1380.23(10)	2301.7(4)	849.82(10)	1412.97(12)	1172.06(8)
c [pm]	744.74(15)	1219.81(9)	1639.7(2)	1157.33(10)	1351.63(10)	2220.46(16)
β [°]	90	97.397(2)	91.806(10)	90	95.837(3)	90.00(2)
V [nm^3]	2.3271	1.40022	2.8306	1.5607	1.4355	2.8939
Z	8	4	8	4	4	8
D_x [Mg/m^3]	1.365	1.893	1.873	1.818	1.911	1.598
μ [mm^{-1}]	3.3	8.5	8.4	7.6	8.3	5.7
F(000)	992	776	1552	840	808	1408
T (°C)	–100	–130	–100	–100	–140	–130
$2\theta_{max}$	50	57.1	50	50	61	60
Refl. measured	4303	14840	9982	2743	30282	34805
Refl. indep.	2160	3559	4974	2743	4374	8849
Transmissions	0.696–0.823	0.208–0.406	0.272–0.994	0.151–0.312	0.479–0.862	0.601–1.000
R_{int}	0.043	0.031	0.069	0.0	0.032	0.039
Parameters	115	125	248	137	134	269
Restraints	0	45	90	161	0	0
wR (F^2, all refl.)	0.072	0.048	0.066	0.089	0.051	0.075
R [F, $>4\sigma(F)$]	0.027	0.021	0.034	0.098	0.020	0.049
S	1.04	0.97	0.71	0.855	1.04	0.99
Max. $\Delta\rho$ (e/nm^3)	368	1496	574	839	703	1649

be obtained free of charge from The Cambridge Crystallographic Data Centre via www.ccdc.cam.ac.uk/data_request/cif.

Acknowledgments

M. B. wishes to thank Prof. W. Thiel for his continuing support and the Deutsche Forschungsgemeinschaft for a Heisenberg fellowship. Computations were performed on Compac XP1000 and ES40 workstations at the MPI Mülheim.

---

[1] R. A. Zingaro, E. A. Meyers, *Inorg. Chem.* **1962**, *1*, 771.

[2] D. J. Williams, K. J. Wynne, *Inorg. Chem.* **1976**, *15*, 1449.

[3] M. D. Rudd, S. V. Lindemann, S. Husebye, *Acta Chem. Scand.* **1997**, *51*, 689.

[4] M. Arca, F. A. Devillanova, A. Garau, F. Isaia, V. Lippolis, G. Verani, F. Demartin, *Z. Anorg. Allg. Chem.* **1998**, *624*, 745; W. W. Schweikert, E. A. Meyers, *J. Phys. Chem.* **1968**, *72*, 1561; D. C. Apperley, N. Bricklebank, S. L. Burns, D. E. Hibbs, *J. Chem. Soc., Dalton Trans.* **1998**, 1289.

[5] W.-W. du Mont, *Main Group Chem. News* **1994**, *2*, 18; M. Bätcher, Ph. D. thesis, University of Oldenburg, **1989**; J. Jeske, Ph. D. thesis, Techn. University of Braunschweig, **1997**.

[6] S. M. Godfrey, S. L. Jackson, C. A. McAuliffe, R. G. Pritchard, *J. Chem. Soc., Dalton Trans.* **1997**, 4499.

[7] J. Jeske, W.-W. du Mont, P. G. Jones, *Chem. Eur. J.* **1999**, *5*, 385.

[8] S. M. Godfrey, S. L. Jackson, C. A. McAuliffe, R. G. Pritchard, *J. Chem. Soc., Dalton Trans.* **1998**, 4201.

[9] E. Seppälä, F. Ruthe, W.-W. du Mont, P. G. Jones, *Chem. Commun.* **1999**, 1471.

[10] (10-Se-3) means: 10 valence electrons at the central Se atom, which has 3 substituents: C. W. Perkins, J. C. Martin, A. J. Arduengo III, W. Lau, A. Alegria, J. K. Kochi, *J. Am. Chem. Soc.* **1980**, *102*, 7753.

[11] W.-W. du Mont, A. Martens von Salzen, F. Ruthe, E. Seppälä, G. Mugesh, F. A. Devillanova, V. Lippolis, N. Kuhn, *J. Organomet. Chem.* **2001**, *623*, 14; W.-W. du Mont, A. Martens von Salzen, F. Ruthe, E. Seppälä, G. Mugesh, F. A. Devillanova, V. Lippolis, N. Kuhn, *J. Organomet. Chem.* **2001**, *628*, 280.

[12] R. Bartsch, O. Stelzer, R. Schmutzler, *Z. Naturforsch., Teil B* **1981**, *36*, 1349.

[13] a) F. Ruthe, W.-W. du Mont, P. G. Jones, *Chem. Commun.* **1997**, 1947; b) F. Ruthe, Ph. D. thesis, Techn. University of Braunschweig, **2004**.

[14] W. McFarlane, D. S. Rycroft, *J. Chem. Soc., Dalton Trans.* **1973**, 2162.

[15] a) N. Kuhn, H. Schumann, G. Wolmershäuser, *Z. Naturforsch., Teil B* **1987**, *42*, 674; b) N. Kuhn, G. Henkel, H. Schumann, R. Fröhlich, *Z. Naturforsch., Teil B* **1990**, *45*, 1010.

[16] H. Duddeck, *Prog. Nucl. Magn. Reson. Spectrosc.* **1994**, *27*, 1–323.

[17] S. W. Carr, R. Colton, *Aust. J. Chem.* **1981**, *34*, 35.

[18] C. Druckenbrodt, Ph. D. thesis, Techn. University of Braunschweig, **2000**.

[19] a) M. Bühl, W. Thiel, U. Fleischer, W. Kutzelnigg, *J. Phys. Chem.* **1995**, *99*, 4000; b) H. Fleischer, S. Glang, D. Schollmeyer, N. W. Mitzel, M. Bühl, *Dalton Trans.* **2004**, 3765.

[20] a) R. C. Binning, L. A. Curtiss, *J. Comput. Chem.* **1990**, *11*, 1206; b) S. Huzinaga, *J. Chem. Phys.* **1965**, *42*, 1293; c) W. J. Hehre, R. Ditchfield, J. A. Pople, *J. Chem. Phys.* **1972**, *56*, 2257; d) P. C. Hariharan, J. A. Pople, *Theor. Chim. Acta* **1973**, *28*, 213; e) T. H. Dunning, *J. Chem. Phys.* **1970**, *53*, 2823; f) A. D. McLean, G. S. Chandler, *J. Chem. Phys.* **1980**, *72*, 5639.

[21] J. R. Cheeseman, G. W. Trucks, T. A. Keith, M. J. Frisch, *J. Chem. Phys.* **1996**, *104*, 5497.

[22] M. J. Frisch, G. W. Trucks, H. B. Schlegel, G. E. Scuseria, M. A. Robb, J. R. Cheeseman, V. G. Zakrzewski, J. A. Montgomery, R. E. Stratman, J. C. Burant, S. Dapprich, J. M. Milliam, A. D. Daniels, K. N. Kudin, M. C. Strain, O. Farkas, J. Tomasi, V. Barone, M. Cossi, R. Cammi, B. Mennucci, C. Pomelli, C. Adamo, S. Clifford, J. Ochterski, G. A. Petersson, P. Y. Ayala, Q. Cui, K. Morokuma, D. K. Malick, A. D. Rabuck, K. Raghavachari, J. B. Foresman, J. Cioslowski, J. V. Ortiz, A. G. Baboul, B. B. Stefanov, C. Liu, A. Liashenko, P. Piskorz, I. Komaromi, R. Gomperts, R. L. Martin, D. J. Fox, T. Keith, M. A. Al-Laham, C. Y. Peng, A. Nanayakkara, C. Gonzalez, M. Challacombe, P. M. W. Gill, B. G. Johnson, W. Chen, M. W. Wong, J. L. Andres, C. Gonzales, M. Head-Gordon, E. S. Replogle, J. A. Pople, *Gaussian98*, Gaussian, Inc., Pittsburgh, PA, **1998**.

[23] **1cA** and **1cB** are very close-lying minima, and seemingly only a small rotation of the *i*Pr group is needed to convert the former into the mirror image of the latter; however, larger reorientations of the interlocking methyl groups from the *t*Bu substituents are involved in this interconversion (not visible from the plot in Scheme 2), and **1cA** and **1cB** are distinct, genuine minima (e.g. they do not collapse into the same one when tighter convergence criteria are applied in the optimisation).

[24] C. D. Rithner, C. H. Bushweller, *J. Am. Chem. Soc.* **1985**, *107*, 7823.

[25] C. D. Rithner, C. H. Bushweller, *J. Phys. Chem.* **1986**, *90*, 5023.

[26] H.-U. Steinberger, B. Ziemer, M. Meisel, *Acta Crystallogr., Sect. C* **2001**, *57*, 323.

[27] M. Freytag, P. G. Jones, *Chem. Commun.* **2000**, *4*, 277.

[28] W. Nakanishi, S. Hayashi, *J. Organomet. Chem.* **2000**, *611*, 178.

[29] W.-W. du Mont, F. Ruthe, *Coord. Chem. Rev.* **1999**, *189*, 101.

[30] M. C. Aragoni, M. Arca, F. Demartin, F. A. Devillanova, A. Garau, F. Isaia, F. Lelj, V. Lippolis, G. Verani, *Chem. Eur. J.* **2001**, *7*, 3122.

[31] F. Bigoli, A. M. Pellinghelli, P. Deplano, F. A. Devillanova, V. Lippolis, M. L. Mercuri, E. F. Trogu, *Gazz. Chim. Ital.* **1994**, *124*, 445.

Received: July 5, 2005